



Pituitary gland under infrared light – in search of a representative spectrum for homogenous regions

Journal:	<i>Analyst</i>
Manuscript ID:	AN-ART-10-2014-001985.R1
Article Type:	Paper
Date Submitted by the Author:	22-Dec-2014
Complete List of Authors:	Banas, Agnieszka; Singapore Synchrotron Light Source, Banas, Krzysztof; Singapore Synchrotron Light Source, National University of Singapore, Furgal-Borzych, Alicja; Jagiellonian University Medical College, Department of Histology Kwiatek, Wojciech; The Henryk Niewodniczanski Institute of Nuclear Physics PAN, Dept. of Applied Physics of Complex Systems Pawlicki, Bohdan; Gabriel Narutowicz Hospital, Breese, Mark; National University of Singapore, Department of Physics; Singapore Synchrotron Light Source, National University of Singapore,

Pituitary gland under infrared light - in search of representative spectrum for homogenous regions

A. Banas^{1*}, K. Banas¹, A. Furgal-Borznych², W. M. Kwiatek³, B. Pawlicki⁴, M.B.H. Breese¹

¹*Singapore Synchrotron Light Source, National University of Singapore, 5 Research Link, Singapore 117603, Singapore*

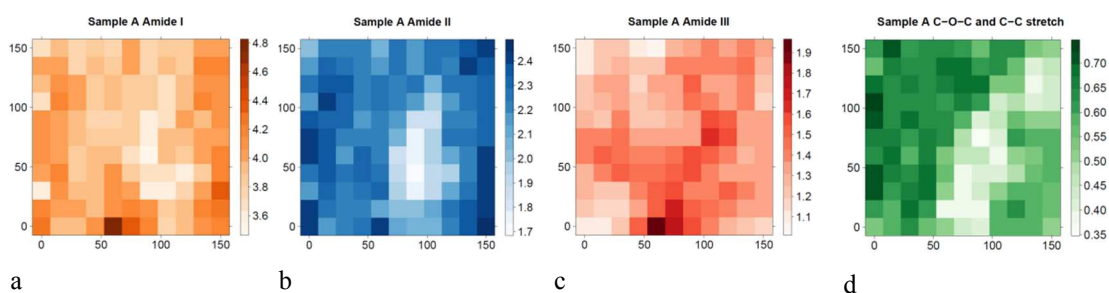
²*Department of Histology, Jagiellonian University Medical College, Kopernika 7, 31-034 Krakow, Poland*

³*Institute of Nuclear Physics PAN, Radzikowskiego 152, 31-342 Krakow, Poland*

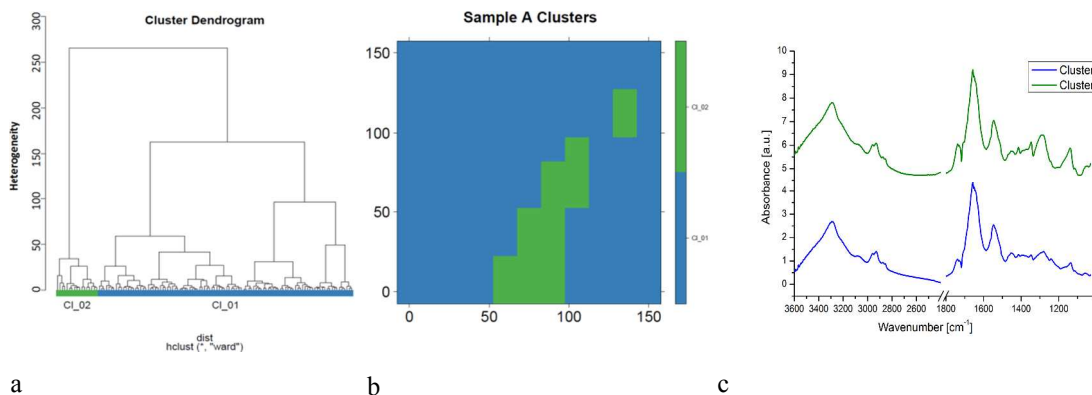
⁴*Gabriel Narutowicz Hospital, Pradnicka 37, 31-202 Krakow, Poland*

*e-mail: slsba@nus.edu.sg

This work focuses on finding unique – representative FTIR spectrum characteristic for one type of cells architecture within the sample. Presented idea is based on using of hierarchical cluster analysis (HCA) for data evaluation to search for uniform patterns within samples from the perspective of FTIR spectra.



Distributions of bands characteristic for Amide I (a), Amide II (b), Amide III (c) and C-O-C and C-C stretching (d) obtained for area selected as Sample A.



Results of HCA analysis applied to FTIR spectra collected for Sample A, presented in form of cluster dendrogram (a), two cluster distributions (b) and average FTIR spectra characteristic for cluster 1 and cluster 2 (c).

Pituitary gland under infrared light – in search of a representative spectrum for homogenous regions

A. Banas^{1*}, K. Banas¹, A. Furgal-Borzych², W. M. Kwiatek³, B. Pawlicki⁴, M.B.H. Breese¹

¹*Singapore Synchrotron Light Source, National University of Singapore, 5 Research Link, Singapore 117603, Singapore*

²*Department of Histology, Jagiellonian University Medical College, Kopernika 7, 31-034 Krakow, Poland*

³*Institute of Nuclear Physics PAN, Radzikowskiego 152, 31-342 Krakow, Poland*

⁴*Gabriel Narutowicz Hospital, Pradnicka 37, 31-202 Krakow, Poland*

*e-mail: slsba@nus.edu.sg

Abstract

The pituitary gland is a small but vital organ in the human body. It is located at the base of the brain and is often described as master gland due to its multiple functions.

The pituitary gland secretes and stores hormones, such as the thyroid-stimulating hormone (TSH), adrenocorticotrophic hormone (ACTH), growth hormone (hGH), prolactin, gonadotropins, and luteinizing hormones, as well as the antidiuretic hormone (ADH). A proper diagnosis of pituitary disorders is of the utmost importance as this organ participates in regulating a variety of body functions. Typical histopathological analysis provides much valuable information, but it gives no insight into the biochemical background of the changes that occur within the gland.

One approach that could be used to evaluate biochemistry of tissue sections obtained from pituitary disorders is Fourier Transform Infra-Red (FTIR) spectromicroscopy.¹

In order to collect diagnostically valuable information large areas of tissue must be investigated.²

This work focuses on finding a unique and representative FTIR spectrum characteristic for one type of cell architecture within a sample. The idea presented is

1
2
3 based on using hierarchical cluster analysis³ (HCA) for data evaluation to search for
4 uniform patterns within samples from the perspective of FTIR spectra. The results
5
6 obtained demonstrate that FTIR spectromicroscopy, combined with proper statistical
7
8 evaluation, can be treated as complementary methods for histopathological analysis
9
10 and ipso facto can increase the sensitivity and specificity for detecting various
11
12 disorders, not only for the pituitary gland, but also for other human tissues.
13
14
15
16
17
18
19
20
21

22 **Introduction**

23
24
25 The pituitary gland is a small bean-shaped organ located at the base of the brain. In
26
27 adults it measures approximately 12 mm in width (transverse diameter, side to side)
28
29 and 10 mm in length (antero-posterior diameter, from front to back). Its height is 5.7
30
31 mm (± 1.7 mm) and never exceeds 10 mm.
32
33

34
35 The pituitary gland has been termed the “master gland” because of the numerous
36
37 hormones that emanate from it and help regulate important functions such as growth,
38
39 blood pressure and reproduction. Pituitary disorders can cause a wide spectrum of
40
41 symptoms, both hormonal and neurological, due to its location near the brain, the
42
43 intracranial nerves and blood vessels and also because of the vital hormonal control
44
45 that the gland provides.⁴ Diagnosis of pituitary disease can be difficult because it is
46
47 often confused with other disorders. The development of better therapeutic strategies
48
49 for pituitary illnesses is complicated by the relative scarcity of human pituitary
50
51 material for basic experimentation. Understanding what exactly happens when the
52
53 pituitary gland starts producing hormones in an uncontrolled way and when it
54
55
56
57
58
59
60

1
2
3 increases its size seems to be extremely important. Such an understanding may also
4
5 help in the selection of reliable treatment options.
6
7

8 Standard histopathological analysis of hematoxylin-and-eosin (H&E) stained pituitary
9
10 sections (performed on post-operative or biopsy material) is still the most popular
11
12 method to assess the malignancy of cells and prepare/predict the proper treatment.
13
14 Undoubtedly histopathological analysis provides much valuable information but it
15
16 lacks quantitative accuracy and gives no account of the biochemical background of the
17
18 changes that occur along with different disorders in the tissue. There remains a need
19
20 for a supplementary method to analyze pituitary samples which could increase the
21
22 sensitivity and specificity of detecting various disorders.
23
24
25
26

27 FTIR spectromicroscopy is a powerful technique which is utilized in many
28
29 applications – it was recently proposed as a rapid, accurate and sensitive technique in
30
31 biomedical research.^{5,6} The FTIR spectrum represents a signature of a sample with
32
33 absorbance or transmittance peaks corresponding to the frequencies of vibrations
34
35 between the bonds of the molecules within the material. FTIR is a useful choice for
36
37 analyzing the distribution of molecular markers in a bio-structure. Using intense
38
39 synchrotron radiation (SR) as a source of infra-red (IR) light, and taking advantage of
40
41 SR properties (high brightness, small effective source size), FTIR spectromicroscopy
42
43 can reach a new dimension in qualitative and quantitative analysis of heterogeneous
44
45 biological samples. It can detect chemical signals on a molecular level within their
46
47 microstructures that could be “invisible” using a Globar source (a silicon carbide rod
48
49 of 5 to 10 mm width and 20 to 50 mm length which is electrically heated) or any other
50
51 conventional IR source. It is worth adding that synchrotron IR light is not destructive,
52
53
54
55
56
57
58
59
60

1
2
3
4 even to the biological samples, as it does not break any bonds or change the inherent
5
6 chemical formula. According to studies performed by Holman et al⁷ focused
7
8 synchrotron IR light increases the temperature of biological samples by about 0.5 K,
9
10 therefore the same samples analyzed by IR can be later examined by other techniques
11
12 (for example X-ray fluorescence - in order to find information about the elemental
13
14 composition).

15
16
17 FTIR spectromicroscopy has been widely used in the analysis of various types of
18
19 pathologically changed tissue samples (cervical^{8,9}, colon^{10,11}, pancreatic¹²,
20
21 prostate^{13,14}, lung¹⁵, breast^{16,17}, glioma^{18,19}) to find clues which could help in following
22
23 the development of the diseases. The main result of all these studies is that normal and
24
25 malignant tissues can be differentiated with an accuracy of around 80 to 100% using
26
27 FTIR combined with statistical methods.
28
29

30
31
32 FTIR analysis on biological samples has to be carried out in cooperation with
33
34 histopathologists as the characteristic changes in the tissue structure accompanying
35
36 disease processes can be observed via staining and microscopic examination of thin
37
38 tissue sections. The histopathologist's guidance is necessary to choose the proper area
39
40 of the tissue prior to FTIR analysis. FTIR spectromicroscopy can be treated as a
41
42 complementary method to histopathological studies of the samples; various patterns of
43
44 the disease which are visible under the microscope can be additionally described by
45
46 their various biochemistry. Human cells are composed mostly of water, proteins,
47
48 nucleic acids, lipids and carbohydrates. Any disease can be seen as a biochemical
49
50 change in one of these components, which can be reflected in a FTIR spectrum as IR
51
52
53
54
55
56
57
58
59
60

1
2
3
4 is sensitive to structural variations and changes of the amount of biochemical
5
6 components on the molecular level.
7

8
9 In order to draw meaningful conclusions (for medical doctors) from FTIR
10
11 experiments, it is necessary “to assign” the correct FTIR spectrum to analyzed
12
13 samples areas - the average one which could serve as a hallmark for particular type of
14
15 tissue e.g. stage of the disease.
16

17
18 However one has to take into account the fact that even sample areas described as
19
20 histologically homogenous are not always biochemically uniform, as it is expected
21
22 that substantial modifications may occur on the molecular level even before visible
23
24 changes become apparent. So finding the representative FTIR spectrum for
25
26 histologically and biochemically homogenous areas is of prime importance.
27

28
29 FTIR experiments performed on selected areas of interest within samples produce a
30
31 huge number of raw spectra, so a significant amount of data processing is required to
32
33 extract the most useful information contained within FTIR spectra. Chemometric
34
35 methods have the ability to analyze the vast spectral datasets and thoroughly
36
37 discriminate among spectra of different samples that show only very small changes.
38
39 Multivariate statistical methods are based on the idea that many non-selective
40
41 variables must be taken into consideration instead of only one variable, and then
42
43 ultimately they are correlated in a multivariate model²⁰ which helps in the analysis,
44
45 especially in cases where large amounts of data are generated.
46
47
48
49

50
51 In this paper we describe a method for finding the representative FTIR spectrum
52
53 characteristic for both histologically and biochemically homogenous sample areas.
54
55 The idea presented is based on using of Hierarchical Cluster Analysis (HCA) for data
56
57
58
59
60

1
2
3
4 evaluation to search for uniform patterns within samples from the perspective of FTIR
5
6 spectra.
7
8
9

10 **Experimental**

11
12 Sample preparation was performed in a controlled environment to eliminate, or at least
13 to minimize, any contamination effects. Samples were obtained by standard
14 microsurgical transnasal resection from adult patients undergoing surgery to remove
15 pathological disorders in the pituitary gland. First, material dedicated for the analysis
16 was frozen in liquid nitrogen to stop all living processes occurring in cells. Then, all
17 specimens were cut into 14 μm thick slices with the use of a cryomicrotome; for
18 spectroscopic measurements each slice was mounted on a Mylar foil (thickness of 1.5
19 μm) and air-dried. For every experimental sample, an adjacent section (of the same
20 thickness) was placed on a microscope glass, and was then stained with H&E dye for
21 histopathological examination.
22
23
24
25
26
27
28
29
30
31
32
33
34
35

36 Pre-studies of the samples were performed using optical microscopy by a
37 histopathologist (all samples were examined by the same person), in order to fully
38 characterize the samples by looking at the shape and size of the cells making up the
39 analyzed tissue and to divide all sections into groups: normal and having a stamp of
40 abnormality.
41
42
43
44
45
46
47

48 FTIR analyses of samples were conducted at the Infrared Spectro/Microscopy
49 beamline (ISMI) at the Singapore Synchrotron Light Source (SSLS). The end-station
50 consists of a Bruker IFS 66v/S FTIR spectrometer coupled to a Hyperion 2000
51 (Bruker Optik, Ettlingen, Germany) IR microscope. As a source of radiation, an
52
53
54
55
56
57
58
59
60

1
2
3
4 internal Globar source, as well as IR synchrotron radiation extracted from the edge
5
6 region of a dipole magnet of the compact superconducting electron storage ring Helios
7
8 2 can be used. Owing to its high flux density, the infrared synchrotron radiation source
9
10 provides a signal-to-noise ratio (SNR) of more than one order higher than the Globar
11
12 source when using a microscopic aperture, thus increasing the minimum detectability
13
14 of samples, which is highly recommended in performed studies.
15
16

17
18 All FTIR spectra from pituitary samples (14 μm of tissue on 1.5 μm of a Mylar foil)
19
20 were collected in transmission mode within the spectral range of 4000-600 cm^{-1} by
21
22 averaging 600 interferograms (scans) per point at a spectral resolution of 4 cm^{-1} using
23
24 an IR microscope equipped with a liquid nitrogen-cooled MCT (mercury cadmium
25
26 telluride) detector and a motorized XY stage. The scanner velocity was set to 100 kHz.
27
28 The interferograms were Fourier transformed by applying a Blackman-Harris 3-term
29
30 apodization and a zero filling factor of 4. The spectral resolution was chosen in order
31
32 to improve the SNR ratio and to guarantee that all prominent bands, even those of
33
34 medium intensity, are clearly apparent in the spectrum.
35
36
37

38
39 FTIR imaging was performed on various areas of pituitary specimens which were
40
41 carefully chosen according to the histopathological assessment of the sample. The 15-
42
43 fold Schwarzschild objective with a numerical aperture of 0.4 was used to image
44
45 selected areas of 165 by 165 μm^2 by scanning the sample point by point in two
46
47 dimensions perpendicular to the beam. At each point a FTIR spectrum was collected,
48
49 with slits set to 15 by 15 μm^2 , as the typical diameter of a biological cell is of this
50
51 order. A video camera enabled an optical overview of the investigated areas to be
52
53 recorded. The spectra were divided by the relevant background spectrum to give a
54
55
56
57
58
59
60

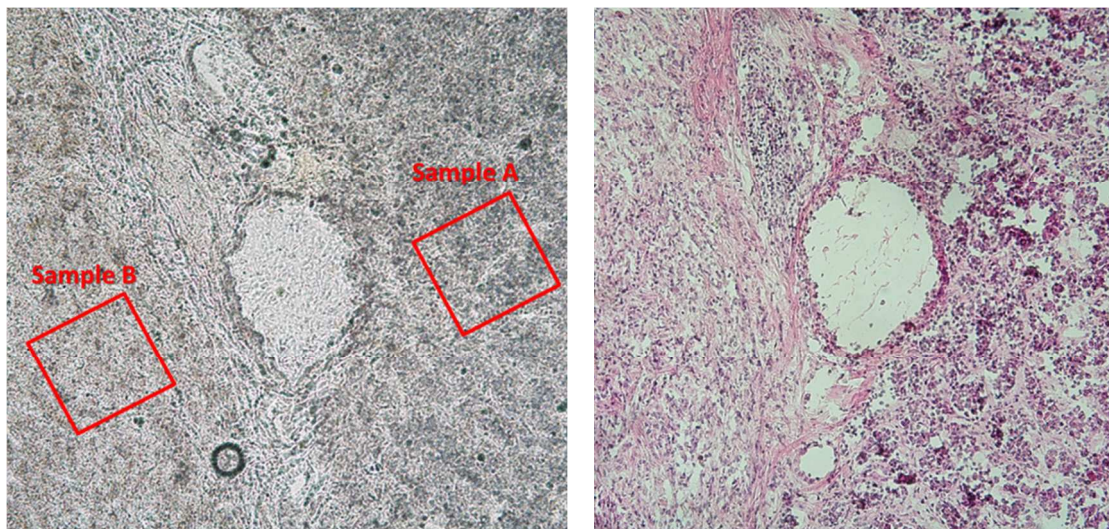
1
2
3 ratio of the transmittance (T) output. All spectra were presented in absorbance units
4
5
6 ($A = -\log T$) as a function of wavenumber (the number of waves per centimeter).
7
8 Background signals were collected from regions of the sample where pure Mylar foil
9
10 was present.

11
12 Spectral data were evaluated using an open source R programming environment for
13
14 statistical analysis, visualization and modelling.²¹ R is the package system which
15
16 allows users to address specific problems with dedicated packages or to create a new
17
18 contribution as a solution in their own fields. In our case additionally, hyperSpec²² and
19
20 ggplot2²³ libraries were loaded in order to perform analysis and visualize the results.
21
22

23
24 The baseline of each FTIR spectrum was corrected using the `spc.fit.poly.below`
25
26 function from the package `hyperSpec`, which calculates iteratively supporting points
27
28 for the baseline polynomials. Then, the spectra were area normalized to eliminate
29
30 spectral differences due to sample thickness.
31
32

33 34 35 **Results and discussion**

36
37 As mentioned in the introduction, the aim of this paper is to present a method for
38
39 obtaining a reliable, informative FTIR spectrum characteristic for a particular cell
40
41 architecture which can be perceived by a histopathologist as a homogenous type of
42
43 tissue. 2-dimensional scans were performed on carefully selected uniform (according
44
45 to the histopathologist) areas within the various types of pituitary tissue disorders. Fig.
46
47 1a shows examples of areas chosen for FTIR measurements – Sample A is marked on
48
49 a glandular part, whereas Sample B is on a nerve part of the unstained layer of a
50
51 pituitary gland removed from the body due to cyst infiltration; Fig. 1b depicts adjacent
52
53 sample stained with the H&E dye.
54
55
56
57
58
59
60



a

b

Fig. 1 Optical microscopic images of pituitary tissue. An unstained sample was prepared for spectroscopic measurements (a) whereas a sample stained with H&E for histopathological assessment (b). Sample A marked on a glandular part and Sample B marked on a nerve part of the pituitary tissue are examples of homogenous (according to histopathological examination) regions selected for FTIR analysis.

Each map consists of 121 FTIR spectra. A typical FTIR spectrum collected for a pituitary sample is presented in Fig. 2.

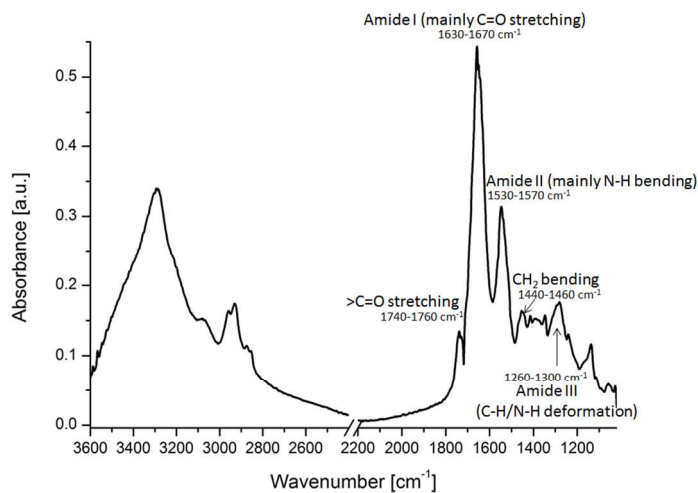


Fig. 2 Typical FTIR spectrum collected for pituitary tissue.

1
2
3
4 The most intense bands in FTIR spectra obtained for pituitary tissue (as for all
5
6 biological systems) belong to proteins, typically they are denoted as Amide I and II.
7
8 Amide I which is composed mainly of C=O stretching bonds, is observed in the
9
10 spectral region $1600\text{--}1700\text{ cm}^{-1}$. This band is very sensitive to small changes in
11
12 hydrogen bonding of the peptide group. Amide II which is represented by a couple of
13
14 N-H in-plane bending and C-N stretching bonds, is found in the spectral region 1480--
15
16 1570 cm^{-1} . According to studies⁵ it is less sensitive to changes and can interfere with
17
18 signals from amino-acid side chains. Weaker protein absorption includes the Amide
19
20 III band at 1254 cm^{-1} .
21
22
23

24
25 Besides protein bands, a FTIR spectrum of pituitary gland tissue consists of a plethora
26
27 of small but informative peaks. This is why it can literally be treated as a mine of
28
29 information of the biochemical status of the analyzed area. As carbohydrates are the
30
31 main energy source of cells, they have their input in a FTIR spectrum. According to
32
33 studies⁵ abnormal cells consume more energy provided by carbohydrates. This should
34
35 be visible as reduced intensities of their bands in a FTIR spectrum collected from
36
37 malignant tissue. Lipids, as being the most prominent constituent of the cells walls,
38
39 play important role in keeping cells in an organized state. Changes in the intensities
40
41 and/or shifts in position of characteristic for lipids bands can manifest an atypical
42
43 separation of the cells or their destruction due to a possible beginning of disorders or
44
45 illness within the pituitary tissue²³. The main spectral characteristic signals of lipids
46
47 and carbohydrates are located in the spectral region $1800\text{--}900\text{ cm}^{-1}$. Nucleic acids
48
49 (DNA and RNA), responsible for carrying information that determine protein
50
51 structure, are represented in a FTIR spectrum mainly as asymmetric and symmetric
52
53
54
55
56
57
58
59
60

phosphate stretching. Assignment of the most prominent absorption bands observed in a typical FTIR spectrum for pituitary tissue presented in Tab. 1.

Tab. 1 Assignment of the most prominent absorption bands observed in a FTIR spectrum collected for a pituitary sample^{5,24}.

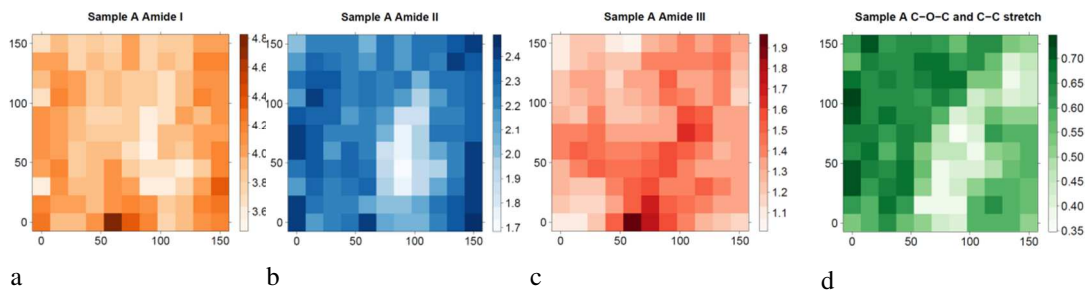
Frequency range [cm ⁻¹]	Type of vibration	Mainly observed in
1740-1760	>C=O stretching	Esters (lipids, phospholipids)
1630-1670	Amide I (mainly C=O stretching)	Proteins
1530-1570	Amide II (mainly N-H bending)	Proteins
1440-1460	CH ₂ bending	Lipids
1380-1420	>C=O stretching vibration of COO ⁻ groups, CH ₃ symmetric bending	Amino acids, lipids
1260-1300	Amide III (C-H/N-H deformation)	Components of proteins
1210-1250	Antisymmetric P=O stretching vibration in phosphodiester	Nucleic acids, lipids
1070-1150	C-O-C and C-C stretching	Carbohydrates, lipids, glycolipids
1070-1090	Symmetric P=O stretching	Nucleic acids in DNA and RNA

The biochemical homogeneity within the selected regions in Fig 1a was checked by generating the distributions of bands, Fig. 3, characteristic for Amide I, II, III and C-O-C and C-C stretching (from the region 1070-1150 cm⁻¹ mainly observed in carbohydrates, lipids and glycolipids).

The distribution images (maps) of selected bands were obtained by detailed analysis of a single FTIR spectrum collected for each point within the chosen area. This analysis included baseline correction, normalization and finally integration of the area under the peak corresponding to the chosen bands (for example for Amide I band integration was done in the spectral range 1630-1670 cm⁻¹). The distribution images are a description of how the parameter (in this case intensity of the selected type of vibration) varies over a surface. As can be seen in Fig. 3 maps obtained for Sample A reveal a rather heterogeneous biochemistry within the region which was originally defined as homogenous - one distinct region seems to emerge, which is noticeable for

1
2
3
4 all distributions. As previously mentioned all FTIR spectra were area-normalized
5
6 during pre-processing, hence this diversity cannot be related to the sample thickness.
7
8 Averaging all FTIR spectra collected for a current map produces an average FTIR
9
10 spectrum in which some biochemical information can be averaged and lost. So, this
11
12 seems an inappropriate way to find the representative FTIR spectrum for an analyzed
13
14 region in this case and generally in almost every case if one deals with biological
15
16 tissue samples.
17
18

19
20 In order to find the most reliable FTIR spectrum for a selected cell architecture it is
21
22 necessary to build a model extracting not only one but all of the most important and
23
24 distinctive features from a single spectrum, and based on this to divide the analyzed
25
26 area into biochemically homogenous regions. Additionally one has to take into
27
28 account that usually in the case of FTIR spectra of biological specimens, differences
29
30 among them are rather tiny, so to assess properly their significance, i.e., to establish
31
32 whether they originate from real modifications or from statistical errors, it is necessary
33
34 to apply an appropriate statistical method.
35
36
37
38
39
40



51 Fig. 3 Distributions of bands characteristic for Amide I (a), Amide II (b), Amide III (c) and C-O-C and
52 C-C stretching (d) obtained for area selected as Sample A.
53
54
55
56
57
58
59
60

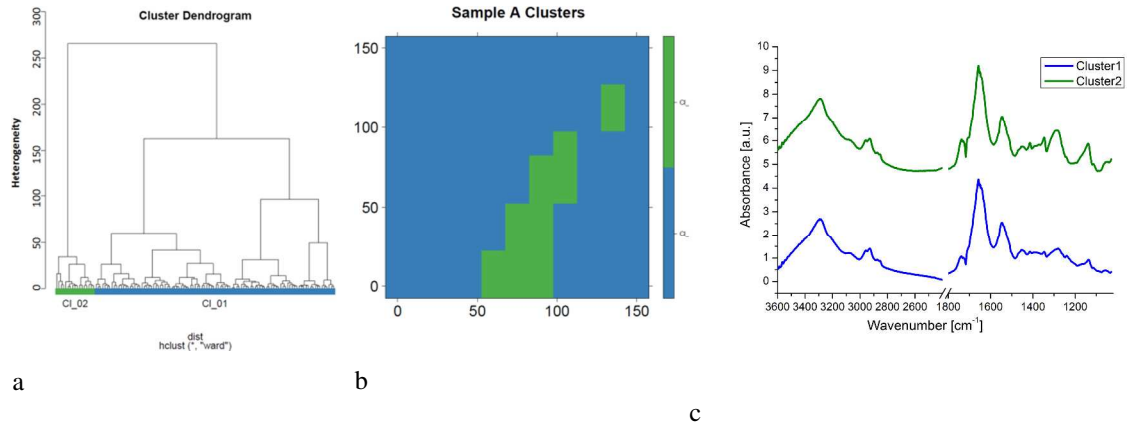


Fig. 4 Results of HCA analysis applied to FTIR spectra collected for Sample A, presented in the form of a cluster dendrogram (a), two cluster distributions (b) and average FTIR spectra characteristic for cluster 1 and cluster 2 (c).

HCA is one of the multivariate statistical methods which is most frequently used to examine the similarity between spectra³. For HCA, each spectrum is treated as a point in n-dimensional measurement space. HCA assesses the similarity between spectra by measuring the distances between the points in the measurement space. Spectra within the same group are more similar to each other than spectra from different groups. HCA is usually applied to data sets for which there is no *a priori* knowledge concerning the class membership of the samples.

HCA was applied to all FTIR spectra collected for 2-dimensional scans on selected areas in order to find representative spectra for biochemically consistent regions. The R platform for statistical computing and graphics was used in the calculations of HCA. As can be seen in Fig. 4a the results which were obtained are not straightforward, the number of clusters strongly depends on the value of heterogeneity (vertical axis) among analyzed spectra. By definition in HCA, the cluster algorithm requires the selection of the number of clusters. It seems to be a very critical decision as selecting various numbers of clusters may lead to various results. Unfortunately, the correct number of clusters is often unknown in advance. In our case, selecting the value of

1
2
3
4 heterogeneity equal to 160 we consider that all spectra are divided into two groups;
5
6 these cluster distributions are presented in Fig. 4b. Two distinct sections are proof that
7
8 our model created two homogenous regions within the analyzed area. A lower value of
9
10 heterogeneity could provide a higher number of clusters, leading to a rather unclear
11
12 classification, so that is why only 2 clusters were taken into account for this example.

13
14 Fig. 4c depicts the average FTIR spectra for each obtained cluster. On carefully
15
16 examining these spectra we can decide whether the differences between them are real
17
18 or are only tiny fluctuations due to experimental errors. Closer inspection of the
19
20 spectra reveals a broad region ranging from 1480 to 1000 cm^{-1} that stands out clearly
21
22 as being different for the obtained clusters. According to Tab. 1 this region contains
23
24 characteristic bands for amino acids, lipids, components of proteins, carbohydrates,
25
26 nucleic acids, glycolipids. Differences in intensities and positions of these lines may
27
28 reveal different biochemical background which can be unique only for one type of cell
29
30 architecture.
31
32
33
34
35

36
37 Similar analysis was performed for the maps collected for Sample B shown in Fig. 1a,
38
39 the area marked on a nerve part of the pituitary tissue. No distinctive features
40
41 comprising more than a few single pixels can be detected in distributions of bands
42
43 characteristic for Amides I, II, III and the C-O-C and C-C stretching bonds presented
44
45 in Fig. 5. This may suggest that this region is indeed homogenous. Results of HCA
46
47 performed on the FTIR spectra indicate that for heterogeneity equal to 55, two clusters
48
49 are found (Fig 6a). This means that analyzed spectra are more similar to each other
50
51 than in the case of FTIR spectra acquired for Sample A. Additionally the cluster
52
53 distribution presented in Fig 6b resembles a kind of mosaic pattern that may indicate
54
55
56
57
58
59
60

that there are very tiny differences between clusters. Mean FTIR spectra obtained for these clusters indeed look very similar, Fig. 6c. Visual inspection cannot reveal any spectral region which differs significantly between the spectra.

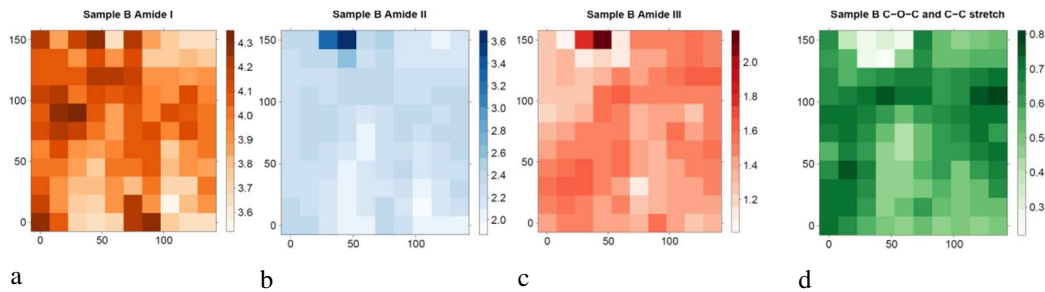


Fig. 5 Distributions of bands characteristic for Amide I (a), Amide II (b), Amide III (c) and C-O-C and C-C stretching (d) obtained for area selected as Sample B.

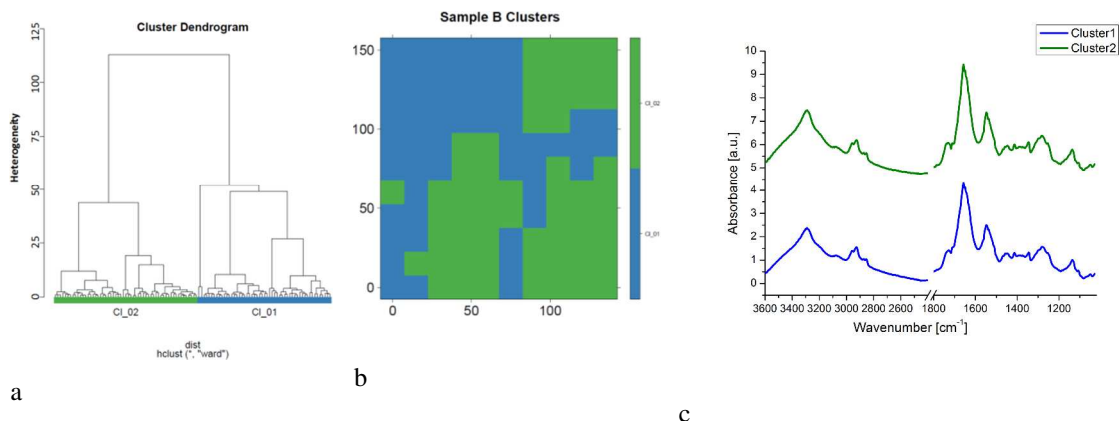
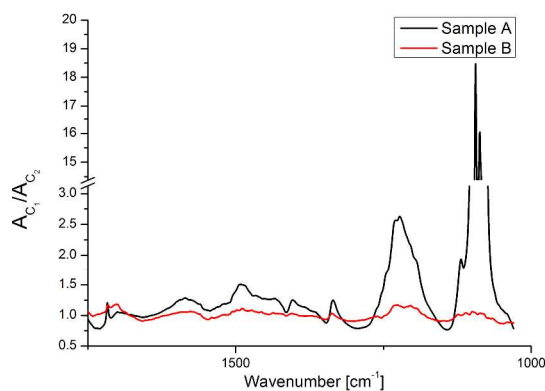


Fig. 6 Results of HCA analysis applied to FTIR spectra collected for Sample B, presented in the form of a cluster dendrogram (a), two cluster distributions (b) and average FTIR spectra characteristic for cluster 1 and cluster 2 (c).

Another way to present clearly the differences between average FTIR spectra which are characteristic of a proper cluster is to calculate the ratio of them, according to the formula: Absorbance for Cluster 1 (A_{C1})/Absorbance for Cluster 2 (A_{C2}). Fig. 7 depicts results of this calculation for clusters found for Sample A and B. As can be seen the highest differences between the average spectra obtained for Cluster 1 and 2 for Sample A are evident within the spectral regions $1280-1140\text{ cm}^{-1}$ and $1140-1030\text{ cm}^{-1}$, where bands typical of nucleic acid, lipids, carbohydrates, glycolipids are

1
2
3
4 present. Lower but also significant alterations can be noticed within the spectral
5
6 regions $1650-1420\text{ cm}^{-1}$, $1410-1360\text{ cm}^{-1}$ and $1340-1320\text{ cm}^{-1}$ where bands typical of
7
8 lipids, proteins, amino acids can be found.
9

10
11 In the case of the average spectrum for Cluster 1 and 2 obtained for Sample B some
12
13 deviations from a ratio equal to 1 can be observed, but they are very small. Based on
14
15 these findings we can assume that Sample B undeniably presents a histologically and
16
17 biochemically homogenous area, while Sample A should be treated as biochemically
18
19 different. Sample B can be described by an average spectrum calculated from all FTIR
20
21 spectra collected for this area, as our analysis proved that Sample A contains two
22
23 different biochemically regions. This is why it can be described by average spectra
24
25 acquired for Cluster 1 and 2.
26
27
28
29
30
31
32



33
34
35
36
37
38
39
40
41
42
43
44
45
46
47 Fig. 7 Ratio of average FTIR spectra characteristic for Cluster 1 and 2. Calculation
48
49 was done for Sample A and B respectively.
50
51
52
53
54
55
56
57
58
59
60

Conclusions

A FTIR spectrum is a unique signature of lipids, proteins, nucleic acids, carbohydrates, etc, which all contribute to its absorption profile. This spectrum reflects a wealth of information about all biological macromolecules making up the sample.

FTIR spectromicroscopy is an extremely sensitive method which allows detection of very small variations within groups of molecules. These variations can be of high significance as they can reveal important changes in biochemistry of pathologically changed tissues and thus contribute to selecting an optimal therapeutic treatment for a suitable disorder. There is a plethora of articles suggesting that FTIR microspectroscopy in conjunction with spectral data processing is a useful approach for diagnostic classification in many diseases, especially various types of cancer. Any information which could be obtained from FTIR spectromicroscopy must be reliable and adequate. Finding the proper FTIR spectrum representative of a histologically and biochemically homogenous tissue area is important. In this manuscript a method of selecting such a spectrum is presented for tissues obtained after pituitary gland resections. However, this scheme is universal and can be applied to the analysis of any 2-dimensional datasets containing FTIR spectra collected for any biological tissues.

The first step in this procedure was the selection of histologically homogenous areas of interest within different cells architecture; this was done by a trained histopathologist. It is common that the biochemical background characteristic for different stages of a disease may not be visible upon examining histopathological tissues, so FTIR mapping was performed on chosen areas in order to obtain their biochemistry status.

1
2
3
4 The second step was the construction of 2-dimensional maps of bands characteristic
5
6 for biological samples - in our case we focused on Amides I, II, III and C-O-C and C-
7
8 C stretching bonds. Closer inspection of band distributions allows for an initial
9
10 assessment of the analyzed area. For biochemically uniform tissue no distinct intensity
11
12 variations among the pixels which make up the maps should be observed. If the pixels
13
14 are grouped it is usually the first indication of different biochemistry within a
15
16 histologically uniform area.
17
18

19
20 The third step was to employ HCA which takes into account information on all chosen
21
22 band distributions to determine the structural characteristics of a data set by dividing
23
24 the data into clusters. As the number of clusters is not known a priori; a decision on
25
26 the number of clusters is usually made after careful assessment of the structure of the
27
28 dendrogram (the graphical output of HCA showing the way that spectra are linked
29
30 together based on their heterogeneity). By checking the value of heterogeneity we
31
32 assumed that for the examples presented in this paper all data can be divided into two
33
34 clusters. However, the final decision about heterogeneity or homogeneity of the
35
36 analyzed area has to be made after examination of the cluster distributions and a
37
38 comparison of their average FTIR spectra. The ratio of Absorbance for Cluster 1 to
39
40 Absorbance for Cluster 2 reveals real similarities or differences between FTIR spectra
41
42 over a broad region of wavenumbers and leads to conclusion about the biochemically
43
44 and histologically homogenous area.
45
46
47
48
49

50 The search for prognostic markers to estimate various types of disease within human
51
52 body tissues is essential for the selection of an optimal therapeutic treatment for
53
54
55
56
57
58
59
60

1
2
3 individual patients. As some disorder types show similar histological characteristics, it
4
5 is important to check their biochemistry.
6
7

8
9 Our study demonstrates that FTIR spectromicroscopy is an ideal method to capture a
10
11 wealth of biochemical information within the tissue sample. However examination of
12
13 different structures and pathological states of biological samples in order to detect and
14
15 monitor changes and structural degeneration requires collection of a huge amount of
16
17 data. It is obvious that visual inspection of the obtained FTIR spectra is not sufficient
18
19 in the evaluation process, thus alternative strategies need to be adopted. FTIR
20
21 spectromicroscopy in combination with hierarchical cluster analysis proved to be well-
22
23 suited for finding a representative spectrum for a histologically and biochemically
24
25 homogenous area. Both methods can be treated as complementary to standard
26
27 histopathological analysis of biological material because they reveal disparity between
28
29 tissue architecture and its biochemical status which can be useful for final diagnosis.
30
31
32
33
34
35
36
37

38 **Acknowledgments**

39 Work partially performed under NUS Core Support C-380-003-003-001.
40
41

42 **References**

- 43 1. L. S. Lee, S.Y. Lin, C.W. Chi, H.C. Liu, C.L. Cheng, *Cancer Lett* , 1995, **94**, 65-69
- 44 2. R. Salzer, H.W. Siesler, 2009, *Infrared and Raman spectroscopic imaging*. Wiley–VCH,
45 Weinheim
- 46 3. C. Krafft, G. Steiner, C. Beleites, R. Salzer, *J Biophotonics*, 2009, **2**(1–2), 13-28
- 47 4. N. Y. Y. Al-Brahim, S. L. Asa *J Clin Pathol*, 2006, **59**, 1245-1253
- 48 5. M. Khanmohammadi, A. B. Garmarudi, *TrAC*, 2011, **30**(6), 864-874
- 49 6. D. Moss, 2010, *Biomedical Applications of Synchrotron Infrared Microspectroscopy*. Royal
50 Society of Chemistry, London.
51
52
53
54
55
56
57
58
59
60

- 1
- 2
- 3
- 4
- 5 7. H. N. Holman, M. C. Martin, W. R. Mckinney, *J Biol Phys*, 2003, **29**, 275–286
- 6
- 7 8. K. R. Bambery, B. R. Wood, M. A. Quinn, D. McNaughton, *Aust. J. Chem*, 2004, **57**, 1139-
- 8 1143
- 9
- 10 9. W. Steller, J. Einenkel, L.-C. Horn, U.-D. Braumann, H. Binder, R. Salzer, C. Krafft, *Anal.*
- 11 *Bioanal. Chem.*, 2006, **384**, 145-154
- 12
- 13 10. P. Lasch, W. Haensch, D. Naumann, M. Diem, *Biochim. Biophys. Acta*, 2004, **1688**, 176-186
- 14
- 15 11. T. Richter, G. Steiner, M.H. Abu-Id, R. Salzer, R. Bergmann, H. Rodig, B. Johannsen, *Vib.*
- 16 *Spectroscopy*, 2002, **28**, 103-110
- 17
- 18 12. Y.-J. Chen, Y.-D. Cheng, H.-Y. Liu, P.-Y. Lin, C.-S. Wang, *Chang Gung Med J.*, 2006, **29**,
- 19 518-527
- 20
- 21 13. R. Bhargava, D.C. Fernandez, S.M. Hewitt, I. W. Levin, *Biochim. Biophys. Acta (BBA)-*
- 22 *Biomembr.*, 2006, **1758**, 830-845
- 23
- 24 14. E. Gazi, J. Dwyer, N. P. Lockyer, J. Miyan, P. Gardner, C. Hart, M. Brown, N. W. Clarke,
- 25 *Biopolymers*, 2005, **77**, 18-30
- 26
- 27 15. Y. Yang, J. Sule-Suso, G. D. Sockalingum, G. Kegelaer, M. Manfait, A. J. El Haj,
- 28 *Biopolymers*, **78**, 2005, 311-317
- 29
- 30 16. H. Fabian, N. A. N. Thi, M. Eiden, P. Lasch, J. Schmitt, D. Naumann, *Biochim. Biophys. Acta*
- 31 *(BBA)-Biomembr.*, 2006, **1758**, 874-882
- 32
- 33 17. L. Zhang, G. W. Small, A. S. Haka, L. H. Kidder, E. N. Lewis, *Appl Spectroscopy*, 2003, **57**,
- 34 14-22
- 35
- 36 18. C. Beleites, G. Steiner, M. G. Sowa, R. Baumgartner, S. Sobottka, G. Schackert, R. Salzer,
- 37 *Vib. Spectroscopy*, 2005, **38**, 143-149
- 38
- 39 19. C. Krafft, S. B. Sobottka, K. D. Geiger, G. Schackert, R. Salzer, *Anal. Bioanal. Chemistry*,
- 40 2007, **387**, 1669-1677
- 41
- 42 20. W. Svante, *J Pharm Biomed Anal*, 1991, **9**, 589–596
- 43
- 44 21. R Core Team, 2013, R: A language and environment for statistical computing. R Foundation
- 45 for Statistical Computing, Vienna, <http://www.r-project.org/>
- 46
- 47 22. C Beleites, V Sergio: hyperSpec: a package to handle hyperspectral data sets in R, R package
- 48 version 0.98-20140523, <http://hyperspec.r-forge.r-project.org>
- 49
- 50 23. H. Wickham. ggplot2: elegant graphics for data analysis. Springer New York, 2009
- 51
- 52 24. P.G. Andrus, *Technol. Cancer Res. Treat.*, 2006, **5**, 157-167
- 53
- 54
- 55
- 56
- 57
- 58
- 59
- 60